16th World Conference on Earthquake Engineering, 16WCEE 2017
Santiago Chile, January 9th to 13th 2017
Paper N° 2195
Registration Code: S-Z1465985442

SEISMIC PERFORMANCE EVALUATION OF COUPLED WALLS USING INNOVATIVE HIGHLY DEFORMABLE COUPLING BEAMS

D. Escolano-Margarit [1], R. Garcia [2], S. Raffoul[3], M. Di Benedetti[4], Iman Hajirasouliha[5], M. Guadagnini[6], K. Pilakoutas[7]

[1] *Marie Curie IF, University of Sheffield, d.escolano@sheffield.ac.uk*
[2] *Research Associate, University of Sheffield, r.garcia@sheffield.ac.uk*
[3] *PhD Student, University of Sheffield, sraffoul1@sheffield.ac.uk*
[4] *Teaching Assistant, University of Sheffield, m.dibenedetti@sheffield.ac.uk*
[5] *Senior Lecturer, University of Sheffield, i.hajirasouliha@sheffield.ac.uk*
[6] *Senior Lecturer, University of Sheffield, m.guadagnini@sheffield.ac.uk*
[7] *Professor, University of Sheffield, k.pilakoutas@sheffield.ac.uk*

Abstract

Reinforced concrete (RC) coupled shear walls are commonly used in the design and construction of high rise buildings located in seismic zones to control drifts at upper storeys. When appropriate degree of coupling is provided, the overall seismic overturning moment is resisted by two mechanisms: i) bending at the base of each wall, and ii) moment of the couple of axial compression/tension forces at the base of each wall, the magnitude of which depends on the shear forces generated at the coupling beams. This shear wall system has proven very effective at controlling damage in structures where coupling beams are detailed to provide high energy dissipation. However, such coupling beams need to transfer high shear forces while undergoing large deformations, which in turn impose strain demands on the concrete well beyond its ultimate strain in compression (usually ε_{cu}=0.35-0.40%). As a result, the potential benefit of very ductile coupling beams able to dissipate large amounts of energy is limited by concrete (crushing) failure.

This paper presents results of an experimental and numerical study on a novel structural system that combines the use of conventional, ductile RC shear walls and coupling beams made of a new, confined Highly Deformable Concrete (HDC). HDC incorporates recycled rubber granules from waste tyres as partial replacement of the mineral aggregates. The inclusion of rubber in HDC increases its deformability in compression (up to ε_{cu}=4-5%), which in turn enhances the ductility and energy dissipation capacity of the coupling beams. Pushover analyses are carried out in OpenSees to compare the seismic performance of building structures fitted with conventional coupled walls and walls using confined HDC coupling beams. The results of the study indicate that, for the same risk scenario, buildings with HDC coupling beams exhibit a better performance, in terms of ductility, displacement and energy dissipation capacity than the conventional RC counterparts.

Keywords: Rubberized Concrete; Coupled Wall; Coupling beam

1. Introduction

Reinforced Concrete (RC) structural coupled walls are commonly used in the design and construction of medium to high rise buildings as a primary lateral force resisting system for wind and seismic loads. This shear wall system has proven very effective at controlling drifts and damage in structures where coupling beams are detailed to provide high energy dissipation. If appropriate degree of coupling is provided, the overall seismic overturning moment is resisted by two mechanisms: i) bending at the base of each wall, and ii) moment of the couple of axial compression/tension forces at the base of each wall, the magnitude of which depends on the shear forces generated at the coupling beams. When this wall system is subjected to large lateral actions (due to earthquakes) the coupling beams are required to transfer high shear forces while undergoing large deformations, which in turn impose strain demands on the concrete well beyond its ultimate axial strain in compression (usually ε_{cu}=0.35-0.40%). Therefore, the performance of the entire lateral resisting system depends on the deformation capacity of the coupling beams, which is limited by concrete failure. During the past few decades research on coupling beams has mainly focused on improving the reinforcement detailing [1][2][3], which led to the development of the typical diagonal reinforcement adopted by current codes. Whilst the use of diagonal reinforcement has proven very effective at resisting shear forces in coupling beams, a large amount of confinement reinforcement is often required, thus complicating constructability. More recently, researchers [4][5][6] have proposed the use of High Performance Fibre Reinforced Concrete to reduce the requirement of confinement reinforcement in the diagonals.

In an attempt to produce more sustainable and environmentally friendly structures, research has focused on the use of recycled vulcanised rubber from end-of-life tyres in concrete. Compared to conventional concrete, rubberised concrete (RuC) exhibits higher deformability, ductility, energy dissipation capacity and vibrational damping [7][8]. However the inclusion of rubber in concrete can lead to a significant reduction in compressive strength [9] [10]. Therefore RuC has been mainly used for non-structural purposes, thus preventing the full exploitation of its unique material properties. This study proposes the use of a new Highly Deformable Concrete (HDC) for the construction of coupling beams. HDC utilises a) recycled rubber particles as partial replacement for both fine and coarse aggregates and b) external FRP confinement to recover the strength to levels required for structural applications whilst maintaining the deformation capacity of RuC. Promising results have been reported for confined rubberised concrete with low contents of rubber at material [11] and structural level [12]. However to date the use of large rubber replacement levels (>60%) in structural applications has not been investigated.

This paper presents and discusses the use of a novel structural system that combines ductile RC shear walls and coupling beams made of a new, Highly Deformable Concrete (HDC). The results of an experimental programme aimed at characterizing the mechanical properties of HDC are reported, along with the preliminary results of a numerical study assessing the effectiveness of the proposed, novel structural system.

2. Experimental characterization of Highly Deformable Concrete (HDC)

The axial stress-strain behaviour of HDC was characterized through monotonic tests on cylinders confined with Aramid Fibre Reinforced Polymer (AFRP). The following section presents the test procedure and discusses the main results.

2.1 Materials

A concrete mix with a 28-day target compressive strength of 60 MPa was used as reference mix (with no rubber). CEM II-52.5 N Portland Limestone Cement was used to reduce the carbon footprint of the concrete. The coarse aggregates were river washed gravel including two sizes (50-10 and 10-20 mm), whereas the fine aggregate was washed river sand (0-5mm). Two different commercial water reducing admixtures were used to

improve workability. Rubber particles of similar sizes were used to replace 60% (by volume) of the fine and 60% of the coarse aggregate for the rubberised concrete mix. Such rubber was obtained from mechanical shredding of vehicular tyres at ambient temperature. The specimens were wrapped with two layers of AFRP using a wet lay-up technique. The fibres were oriented perpendicular to the main axis of the cylinders and an overlap of 100mm was used to guarantee adequate anchorage of the AFRP sheet. The properties of the unidirectional AFRP dry fibres used in this study are the following: tensile strength f_f=2400 MPa, modulus of elasticity E_f=116GPa, ultimate elongation ε_{fu}=2.5%, and thickness of sheet t_f=0.29 mm.

2.2. Test set-up and instrumentation

All specimens were tested in a 3000 kN capacity compression machine with a loading rate of 2 MPa/min. The load was monotonically increased under force control up to failure. To prevent crushing of the concrete due to stress concentration, the top and bottom of the cylinders were confined using high-strength high-ductility Post Tensioned Metal Straps (PTMS) of thickness 0.8 mm and width 13 mm [13]. Fig. 1 shows the final set up during the test. Deformations in axial and horizontal directions were measured locally and globally. At the global level, 3 LVDTs measured the axial deformation between two parallel rings attached to the cylinder. Horizontally a pre-tensioned wire around the central section of the cylinder measured the lateral expansion of the specimens at mid-height. Five 120Ω strain gauges measured the vertical and lateral strains on the AFRP jacket. Three gauges were mounted in the horizontal (H) direction and two in the vertical (V) direction. H3 was placed in the middle of the overlap, while H1 and H2 were distributed following a 120 degree angle (see Fig. 2). Vertical gages V1 and V2 were placed in the section perpendicular to H3. Fig. 2 shows the instrumentation layout.

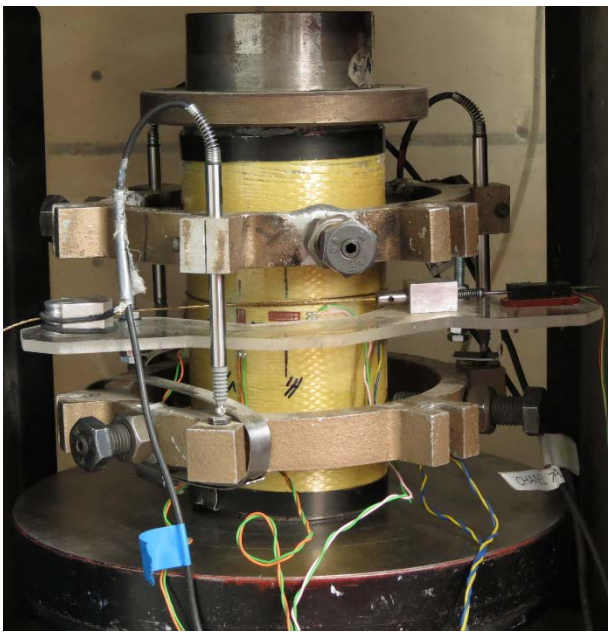

Fig. 1 Set-up

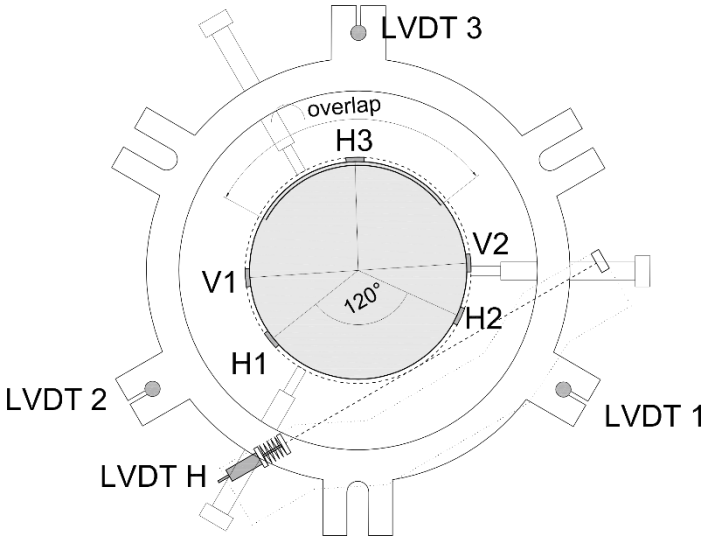

Fig. 2 - Instrumentation

2.3. Results and discussion

All specimens (except specimen AFRP-SP1) failed in an explosive manner following rupture of the AFRP jacket at the central part of the cylinders at a lateral strain close to the ultimate strains of the fibres (21,000 με). Table 1 summarises the main results obtained during the tests, where f_c is the unconfined compressive strength, f_{cy} is the axial compressive yield strength, f_{cc} is the confined compressive strength, ε_{cy} is the axial yield strain, ε_{cu} is the axial ultimate strain, E_c is the modulus of elasticity before yielding, f_{cc}/f_c is the confinement effectiveness, and $\varepsilon_{cu}/\varepsilon_{cy}$ is the ductility. In specimen AFRP-SP1 the metal straps failed prematurely, thus reducing the maximum expected values.

Fig. 3 shows the stress strains relationship for the tested specimens. As can be seen in Fig. 3 HDC has a bilinear shape similar to that of regular FRP confined concrete with two distinct linear parts, connected by a transition zone: 1) an initial elastic part controlled by the unconfined behaviour of RuC until the material reaches the yield strength f_{cy} followed by a curved transition zone; and 2) a second linear part controlled by the lateral expansion of the AFRP jacket.The results indicate that confining RuC with an AFRP jacket recovered the compressive strength of the RuC up to 7.7 times the initial strength, thus making this HDC suitable for structural applications. In terms of axial strain, confining with two layers of AFRP enhanced the concrete deformation capacity and achieved strains of up to 4.6%. This level of strain corresponds to approximately 20 times the strain at maximum strength of conventional concrete with no rubber.

Table 1 - Experimental results

cylinder ID	*# layers*	f_c *(MPa)*	f_{cy} *(MPa)*	f_{cc} *(MPa)*	ε_{cy} *(μm)*	ε_{cu} *(μm)*	E_c *(GPa)*	f_{cc}/f_{c0}	$\varepsilon_{cu}/\varepsilon_{cy}$
UNCONFINED	0	7.81	n/a	n/a	n/a	n/a	9.8	n/a	n/a
AFRP-SP1	2	n/a	10.89	41.05	1031	27860	10.58	5.6	27
AFRP-SP2	2	n/a	8.67	49.8	894	37390	10.06	6.8	42
AFRP-SP3	2	n/a	9	56.2	928	46610	9.9	7.7	50

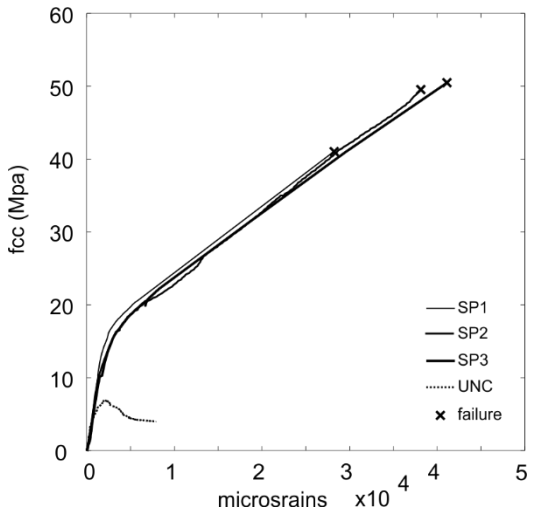

Fig. 3 - Stress Strain Relationship

3. Numerical study

3.1. Prototypes and FE models

A prototype of a typical housing building of 6 storeys was considered in this study (Fig. 4). The tributary vertical load on the walls corresponded to a 6x6 m span with a permanent action of G=6 kN/m^2 and a variable action of Q=2 kN/m^2. The walls dimensions were selected to ensure an axial design load of N_d =0.1 N_{max} (where N_{max} is the ultimate axial strength and N_d is the axial design load). The longitudinal flexural reinforcement was designed to satisfy Eurocode 8 [14] and Eurocode 2 [15]. A capacity design was used to design transversal shear reinforcement, thus forcing a flexural failure mode. For the coupling beams a shear dominated failure mode was considered, and therefore the length to depth ratio was kept smaller than 3.

The prototypes were modelled in OpenSees [16], [17] using 2D linear elements (Fig. 4). The walls were modelled using fibre section elements with distributed plasticity. These elements are suitable for coupled wall systems, as they capture the moment-axial interaction as well as the axial elongation due to flexure [18]. The coupling beams were modelled using diagonal trusses defined with fibre sections [19]. This model considers the contribution of the confined concrete core along with that of the diagonal reinforcement [20]. The compression struts and tension ties were defined by the stress-strain relationship of the concrete and steel respectively. The experimental curves obtained from the cylinder tests described in section 2 were used to model the behaviour of HDC. The experimental results of tests carried out by Naish et al [21] on a conventional concrete coupling beam were used to validate the numerical model (Fig. 5). Finally, the coupling beams were connected to the shear walls through rigid elements.

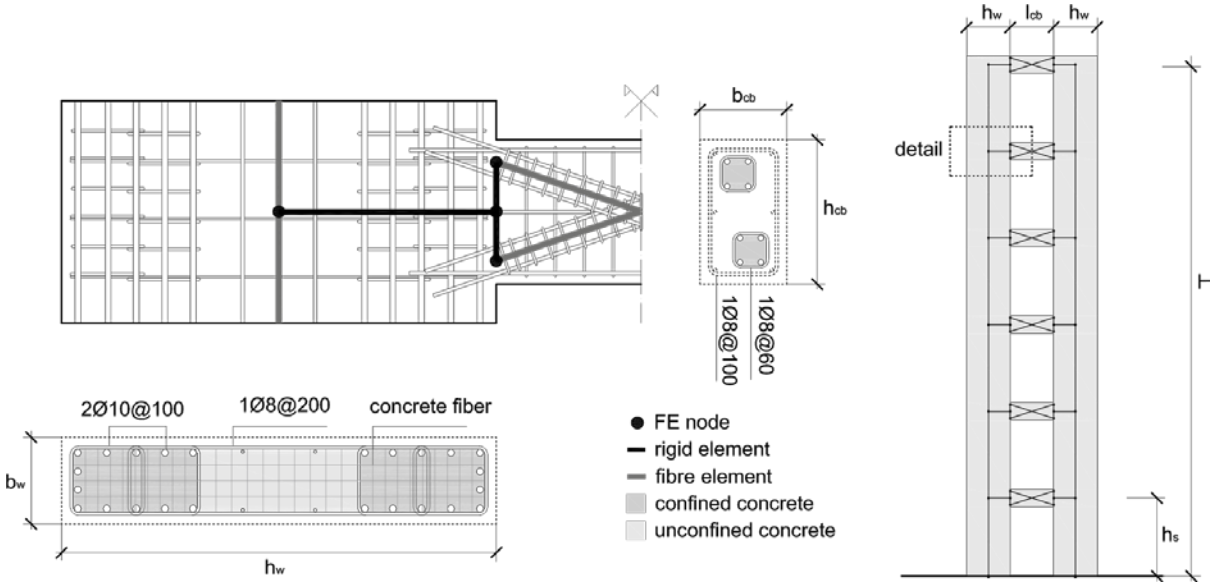

Fig. 4 - Typical prototype and FE model definition

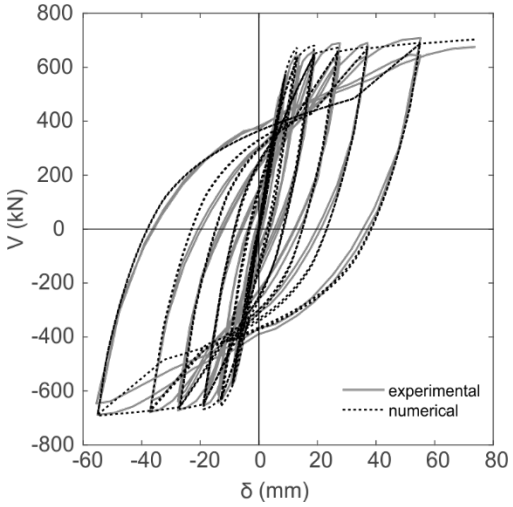

Fig. 5 – Shear force vs displacement hysteretic curve

3.2. Push over analyses

Similarly to the work done by Inoue & Kuwahara [22] a relationship between the relative stiffness and the coupling ratio is defined here to compare the performance of both structural system. The coupled wall system

was idealised as an elastic perfectly plastic system (Fig. 6), where the bending moment at the base of the overall system, M_{y0}, the walls, M_w and the coupling action, M_{cb} , is plotted against the drift of the top story, θ. Two parameters define this structural system: (i) the relative stiffness ratio, K, which is the ratio between the stiffness of the coupling system, k_{cb}, and the stiffness of the wall system, k_w, (as defined in Eq. (1)); and (ii) the coupling ratio, β, which is the ratio between the overturning moment resisted by the coupling action, M_{cb}, generated by the accumulation of shear force at the coupling beams, and the overall overturning moment (Eq. (2)).

$$\boldsymbol{K = \frac{k_{cb}}{k_w}} \tag{1}$$

$$\boldsymbol{\beta = \frac{M_{cb}}{M_{y0}}} \tag{2}$$

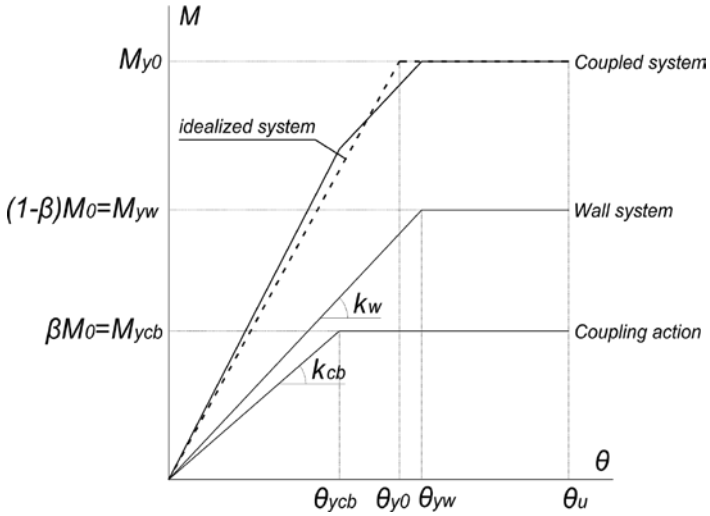

Fig. 6 – EPP idealization of the structural system

The cumulative plastic deformation ratio, η in Eq. (3), along with the ductility, μ in Eq. (4), are two fundamentals parameters when defining the inelastic response of structures. η is a normalised expression of the inelastic strain energy and it can be considered as a measure of damage in a structural element or system [23].

$$\boldsymbol{\eta = \frac{E_p}{M_y \theta_y}} \tag{3}$$

$$\boldsymbol{\mu = \frac{\theta_u}{\theta_y}} \tag{4}$$

where E_p is the inelastic plastic energy, M_y is the yielding moment, θ_y is the yielding rotation, and θ_u is the ultimate rotation.

The cumulative plastic deformation ratio can be expressed as a function of the coupling ratio and the relative stiffness for a certain value of wall ductility as follows.

$$\boldsymbol{\eta = \frac{E_{pw} + E_{pcb}}{M_{y0}\theta_{y0}} = \frac{\theta_{yw}(\mu_w - 1)(1-\beta)M_{y0} + \theta_{cb}(\mu_{cb} - 1)\beta M_{y0}}{M_{y0}\theta_{y0}}} \tag{5}$$

The yielding rotation, θ_{y0}, of the system can be obtained from the idealized bilinear M-θ relationship represented in Fig. 6 with a dash line. The idealized curve of the elastic perfectly plastic system was derived by

imposing that the areas below the original and idealized curves are equal, as proposed in EC8, and the yielding rotation can be calculated as:

$$\theta_{y0} = \theta_{yw}\left(\beta\left(1 - \frac{\mu_w}{\mu_{cb}}\right) - 1\right) \quad (6)$$

From Fig. 6 the following relationships also apply:

$$\theta_u = \mu_{cb}\theta_{ycb} = \mu_w\theta_{yw} \quad (7)$$

$$\eta = K\frac{\mu_w}{\mu_{cb}} \quad (8)$$

From Equations (5) to (8) the cumulative plastic deformation ratio of the coupled wall system can be expressed as:

$$\eta = \frac{-\mu_w}{\beta\left(1 - \frac{\beta}{K(1-\beta)}\right) - 1} \quad (9)$$

With the above relationship in mind, the following section summarises the outcome of a pushover analysis study performed to assess the performance of a conventional coupled wall and the proposed structural system.

3.3. Results

A parametric study was carried out to compare the performance under lateral load of two coupled wall systems: 1) with coupling beams made of conventional RC and 2) with coupling beams made of HDC. The response of both structural systems was compared for different values of K and a constant coupling ratio β=0.3. Table 2 summarises the results of the models considered in this study. The results show that the aspect ratio of the coupling beams and the reinforcement ratio of the coupling beams/walls varied among the different prototypes to obtain the required levels of β and K. The structural performance was analysed up to lateral drift of 1%, which is representative of a Life Safety performance level [24]. Fig. 7 shows a typical pushover curve of both structural systems, for a β=0.3 and K=0.5. The bending moment at the base of the coupled wall system, the walls and the coupling action ($M_{cb} = \sum Vi\,(h_w + l_{cb})$, where V_i is the shear force at the coupling beams of each story) is plotted against the top drift. As can be seen, although different materials and aspect ratio were used for conventional concrete and HDC coupling beams, the demand over the shear wall is practically the same.

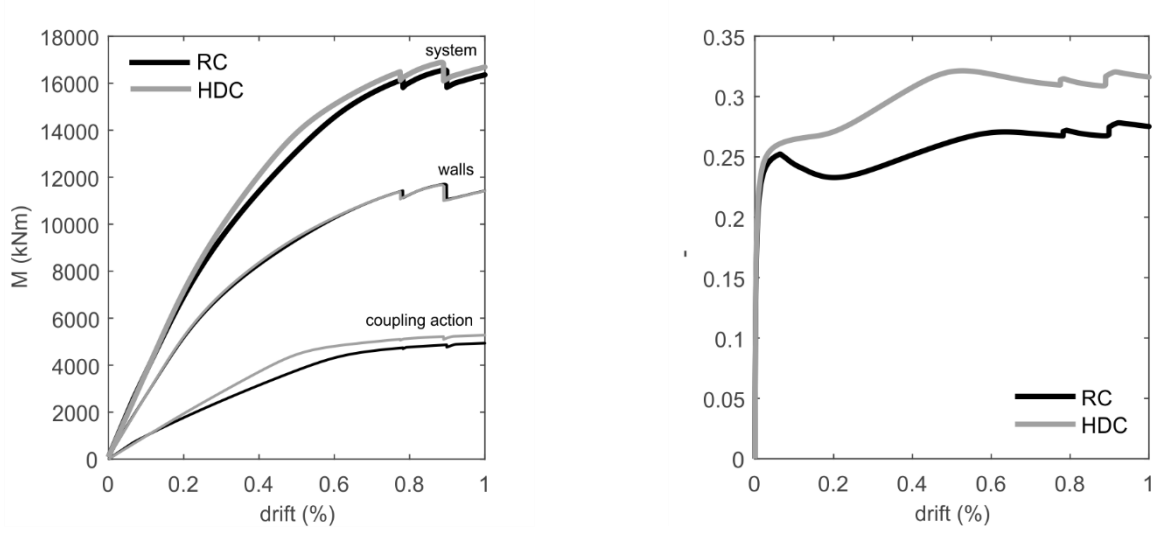

Fig. 7 – Push-Over curve

Fig. 8 - Evolution of the Coupling Ratio

Table 2 - Prototypes properties

h_w (m)	b_w (m)	ρ_w	l_{cb} (m)	h_{cb} (m)	b_{cb} (m)	ρ_{cb}	θ_{yw} (%)	M_{yw} (kNm)	θ_{ycb} (%)	M_{ycb} (kNm)	θ_{y0} (%)	M_{y0} (kNm)	μ_w	η_w	μ_{cb}	η_{cb}	μ_0	η_0	K	β
2	0.3	0.009	1.2	0.4	0.3	0.021	0.49	9090	0.61569	3642	0.52	12732	2.3	1.3	1.8	0.8	2.1	1.1	0.32	0.29
2	0.3	0.013	1.2	0.4	0.3	0.021	0.60	11786	0.65724	4962	0.61	16749	1.9	0.9	1.7	0.7	1.8	0.8	0.38	0.30
2	0.3	0.013	1.2	0.45	0.3	0.019	0.70	15739	0.54118	6315	0.65	22053	1.6	0.6	2.1	1.1	1.7	0.7	0.52	0.29
2	0.3	0.013	1.2	0.5	0.3	0.017	0.68	15737	0.47484	7636	0.62	23373	1.6	0.6	2.3	1.3	1.8	0.8	0.69	0.33
2	0.3	0.006	1.2	0.45	0.3	0.019	0.42	9089	0.53951	3625	0.45	12714	2.7	1.7	2.1	1.1	2.5	1.5	0.31	0.29
2	0.3	0.009	1.2	0.5	0.3	0.017	0.53	11785	0.55417	5341	0.54	17126	2.1	1.1	2.0	1.0	2.1	1.1	0.43	0.31
2	0.3	0.009	1.2	0.55	0.3	0.015	0.52	11793	0.45346	5349	0.50	17142	2.1	1.1	2.4	1.4	2.2	1.2	0.52	0.31
2	0.3	0.013	1.2	0.55	0.3	0.015	0.62	15752	0.46179	7839	0.57	23591	1.8	0.8	2.4	1.4	2.0	1.0	0.67	0.33

For nomenclature refer to Fig 4 and section 3.2

Fig. 8 shows the coupling ratio β versus drift. It is shown that for normal RC coupling beams, the coupling ratio decays as the displacement demand increases up to the point where both wall and coupling beams yield. This is due to a larger stiffness degradation in the coupling beams compared to the walls [25]. By contrast, for HDC coupling beams the coupling ratio increases with the displacement demand. This can be attributed to the lower stiffness degradation and the higher deformation capacity of HDC. Fig. 9 shows the cumulative plastic deformation ratio at the coupling beams for the structural systems at different values of K. It is shown that, for the cases analysed in this study and for the same level of drift, the normalized energy dissipated by the coupling beams with HDC is up to 20% higher than that in RC coupling beams.

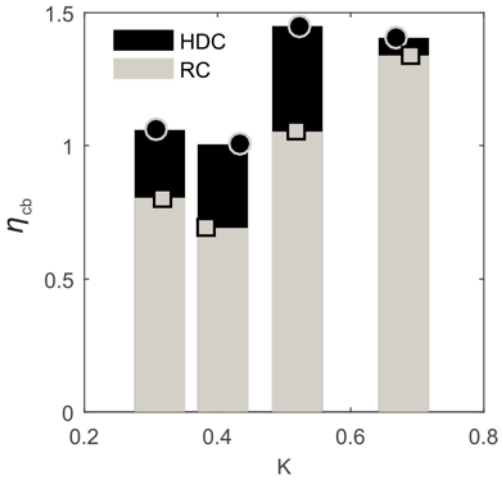

Fig. 9 η in coupling beams for β=0.3

4. Conclusions

The main goal of this study was to evaluate a novel structural system that combines ductile RC shear walls and coupling beams designed with a new Highly Deformable Concrete (HDC). The new structural system was evaluated through numerical pushover analyses. The models were calibrated using multi-scale experimental results at the material (small scale) and structural element level. Although further experimental work to study the effectiveness of the confinement on large scale RuC rectangular elements needs to be done, based on the results of this study, the following conclusions can be drawn:

- Confining rubberized concrete with a 2 layer AFRP jacket recovered the compressive strength of the rubberized concrete up to 7.7 times (f_{cc}=40-60 MPa) the initial strength, thus making HDC suitable for structural applications.
- Axial strains of up to 4.6% (20 times more than conventional concrete) can be achieved when confining rubberised concrete with 2 layers of AFRP.
- Modelling coupling beams using a pair of diagonal trusses provides an accurate estimation of their overall cyclic load deflection relationship.
- The coupling ratio in structural systems with HDC coupling beams increases with the displacement demand, due to the lower stiffness degradation and the higher deformation capacity of HDC.
- For the same performance level, the normalized energy dissipated by the coupling beams made of HDC is up to 20% higher than that dissipated by conventional RC coupling beams.

4. Acknowledgements

The authors would like to thank the financial support provided by the EU H2020 Marie Skłodowska-Curie Programme grant agreement n. 658248 (SHDS project) and the EU 7th Framework Programme grant agreement n. 603722 (Anagennisi project).

5. References

[1] Paulay, T., & Binney, J. R. (1974). Diagonally reinforced coupling beams of shear walls. *ACI Special Publication*, **42**, 579-598.

[2] Tassios, T. P., Moretti, M., & Bezas, A. (1996). On the behavior and ductility of reinforced concrete coupling beams of shear walls. *ACI Structural Journal*, **93**, 711-720.

[3] Galano, L., & Vignoli, A. (2000). Seismic behavior of short coupling beams with different reinforcement layouts. *ACI structural Journal*, **97**(6), 876-885.

[4] Canbolat, B. A., Parra-Montesinos, G. J., & Wight, J. K. (2005). Experimental study on seismic behavior of high-performance fiber-reinforced cement composite coupling beams. *ACI Structural Journal*, **102** (1), 159.

[5] Lequesne, R. D., Parra-Montesinos, G. J., & Wight, J. K. (2012). Seismic Behavior and Detailing of High-Performance Fiber-Reinforced Concrete Coupling Beams and Coupled Wall Systems. *Journal of Structural Engineering*, **139**(8), 1362-1370.

[6] Park, W. S., & Yun, H. D. (2011). Seismic performance of pseudo strain-hardening cementitious composite coupling beams with different reinforcement details. *Composites Part B: Engineering*, **42**(6), 1427-1445.

[7] Al-Tayeb, M. M., Bakar, B. A., Ismail, H., & Akil, H. M. (2013). Effect of partial replacement of sand by recycled fine crumb rubber on the performance of hybrid rubberized-normal concrete under impact load: experiment and simulation. *Journal of Cleaner Production*, **59,** 284-289.

[8] Mohammed, B. S. (2010). Structural behavior and m–k value of composite slab utilizing concrete containing crumb rubber. *Construction and Building Materials*,**24** (7), 1214-1221.

[9] Güneyisi, E., Gesoğlu, M., & Özturan, T. (2004). Properties of rubberized concretes containing silica fume. *Cement and Concrete Research*, **34**(12), 2309-2317.

[10] Topçu, İ. B., & Bilir, T. (2009). Experimental investigation of some fresh and hardened properties of rubberized self-compacting concrete. *Materials & Design*, **30**(8), 3056-3065.

[11] Youssf, O., ElGawady, M. A., Mills, J. E., & Ma, X. (2014). An experimental investigation of crumb rubber concrete confined by fibre reinforced polymer tubes. *Construction and Building Materials*, **53**, 522-532.

[12] Youssf, O., ElGawady, M. A., & Mills, J. E. (2016). Static cyclic behaviour of FRP-confined crumb rubber concrete columns. *Engineering Structures*, **113**, 371-387.

[13] Garcia, R., Helal, Y., Pilakoutas, K., & Guadagnini, M. (2015). Bond strength of short lap splices in RC beams confined with steel stirrups or external CFRP.*Materials and Structures*, **48**(1-2), 277-293.

[14] Eurocode 8: Design of structures for earthquake resistance-Part 1: General rules, seismic actions and rules for buildings. (2005).

[15] Eurocode 2: Design of Concrete Structures: Part 1-1: General Rules and Rules for Buildings. (2004).

[16] Mazzoni, S., McKenna, F., Scott, M. H., & Fenves, G. L. (2006). OpenSees command language manual. *Pacific Earthquake Engineering Research (PEER) Center*.

[17] McKenna, F., Scott, M.H., and Fenves, G.L.. "Nonlinear Finite Element Analysis Software Architecture Using Object Composition." *Journal of Computing in Civil Engineering*, **24**(1):95-107, January 2010.

[18] Paulay, T. (2002). The displacement capacity of reinforced concrete coupled walls. *Engineering Structures*, **24**(9), 1165-1175.

[19] Fox, M., Sullivan, T., & Beyer, K. (2014). Comparison of force-based and displacement-based design approaches for RC coupled walls. *New Zealand. Bulletin of the New Zealand Society for Earthquake Engineering*, **47**, 190-205.

[20] Hindi, R. A. & Hassan, M. A. (2004). Shear capacity of diagonally reinforced coupling beams. *Engineering structures*, **26**(10), 1437-1446.

[21] Naish D., Fry, A.,Klemencic, R & Wallace, J. (2013). Reinforced Concrete Coupling Beams—Part I: Testing. *ACI Structural Journal*, **110**(6), 1057-1066. https://nees.org/warehouse/project/1100.

[22] Inoue, K., & Kuwahara, S. (1998). Optimum strength ratio of hysteretic damper. *Earthquake engineering & structural dynamics*, **27**(6), 577-588.

[23] Akiyama, H. (1985). Earthquake-resistant limit-state design for buildings. University of Tokyo Press.

[24] FEMA, Prestandard. Commentary for the Seismic Rehabilitation of Buildings. *FEMA-356, Federal Emergency Management Agency, Washington, DC*, 2000.

[25] Harries, K. A. (2001). Ductility and deformability of coupling beams in reinforced concrete coupled walls. *Earthquake Spectra*, **17**(3), 457-478.